

EMITTANCE COMPENSATION STUDIES OF PHOTOINJECTOR BEAMS WITH ANGULAR MOMENTUM*

S. Lidia, LBNL, Berkeley, CA 94720, USA

Abstract

Beam dynamics studies on the FNPL photoinjector that seek to optimize the transport of intense electron beams with large values of canonical angular momentum have been performed. These studies investigate the effect of solenoid emittance compensation on beams that evolve under the combined influence of intense space charge forces and large angular momentum. We present details of experimental measurements and supporting simulations of beam envelope evolution.

INTRODUCTION

Flat beams generated in rf photoinjectors have been proposed for the generation of short-pulse hard x-rays [1] based on earlier studies for linear collider applications [2]. The flat beams are generated by a technique that uses a magnetized cathode to create strong coupling between the horizontal and vertical phase spaces. The coupling is removed downstream by a skew quadrupole lattice which produces a beam with large ratio between the vertical and horizontal emittances.

Emittance compensation techniques [3][4] are now widely used in the design and operation of photoinjectors to minimize the normalized emittance of the beam as it is transported from the injector. Here, we study the modifications of the technique for beams that carry large amounts of angular momenta .

THEORETICAL DEVELOPMENT

Emittance

In an azimuthally symmetric system, the normalized 4-D transverse emittance can be expressed as [5]

$$\epsilon_{4D} = \frac{1}{4}(\gamma\beta)^2 \left[\langle r^2 \rangle \langle r'^2 \rangle + \langle r\theta' \rangle^2 - \langle r \cdot r' \rangle^2 - \langle r^2 \theta'^2 \rangle \right] \quad (1)$$

where $r' = dr/dz$ and $\theta' = d\theta/dz$. This emittance measures the volume of the full 4-D transverse phase space. Photoinjector beams can be classified as rigid rotators such that θ is constant over all radii. In this case, the normalized radial emittance

$$\epsilon_{nr} = \frac{1}{2}(\gamma\beta)^2 \left[\langle r^2 \rangle \langle r'^2 \rangle - \langle r \cdot r' \rangle^2 \right] \quad (2)$$

provides the full measure of the beam phase space.

Beam Envelope Evolution

The envelope equation of the RMS radial beam spot size ($\sigma_r = \sqrt{\langle r^2 \rangle}$) can be expressed as [5]

$$\sigma_r'' + \sigma_r' \left(\frac{\gamma'}{\gamma\beta^2} \right) + k_{eff}^2 \sigma_r - \frac{\kappa_s}{\sigma_r} - \frac{\epsilon_{nr}^2}{\sigma_r^3 \gamma^2 \beta^2} - \left(\frac{\langle p_\theta \rangle}{mc\gamma\beta} \right)^2 \frac{1}{\sigma_r^3} = 0 \quad (3)$$

The effective linear restoring force

$$k_{eff}^2 = \frac{\gamma''}{2\gamma\beta^2} + \left(\frac{qB_s}{\gamma\beta mc} \right)^2 \quad (4)$$

depends on both the external magnetic focusing as well as acceleration. The normalized, radial emittance (5th term) and angular momentum (6th term) contribute similarly to the envelope evolution so that an effective emittance can be defined as

$$\epsilon_{eff}^2 = \epsilon_{nr}^2 + \frac{\langle p_\theta \rangle^2}{(mc)^2} \quad (5)$$

The (conserved) canonical angular momentum for a single electron at the point of emission from the cathode is

$$p_\theta = -\frac{1}{2} eB_{z0} r_0^2 \quad (6)$$

and the perveance term describing space charge defocusing is

$$\kappa_s = \frac{I_b / I_0}{(\gamma\beta)^3} \quad (7)$$

Typically, the local thermal emittance in a photoinjector beam is much smaller than the projected emittance that incorporates longitudinal (slice) variations. In our case, we assume that the effective emittance is dominated by correlated angular momentum and that the thermal contribution is completely negligible.

In the absence of acceleration, an equilibrium (laminar) solution to equation (3) is readily found,

$$\sigma_{eq}^2 = \left(\frac{\kappa_s}{2k_{eff}^2} \right) \left[1 + (1 + \mu^2)^{1/2} \right], \quad (8)$$

where

$$\mu = 2 \frac{k_{eff} \epsilon_{eff}}{\gamma\beta\kappa_s} \quad (9)$$

measures the relative influence between the perveance and the effective emittance in describing the envelope dynamics. For space-charge dominated beams μ approaches zero, while for emittance dominated beams μ approaches infinity.

The evolution to the envelope equation linearized about the laminar envelope admits oscillatory solutions with characteristic wavenumber

$$k_{eq}^2 = k_{eff}^2 \left\{ 1 + \frac{2}{\left[1 + (1 + \mu^2)^{1/2} \right]} + \frac{3\mu^2}{\left[1 + (1 + \mu^2)^{1/2} \right]^2} \right\} \quad (10)$$

This wavenumber takes the limiting forms for space-charge dominated and effective-emittance dominated beams,

$$k_{eq}^2 \Rightarrow \begin{cases} 2k_{eff}^2, & \mu^2 \rightarrow 0 \\ 4k_{eff}^2, & \mu^2 \rightarrow \infty \end{cases} \quad (11)$$

*This work was supported by the Department of Energy under Contract No. DE-AC03-76SF00098.

When acceleration is included, these same formulae apply to describe new equilibria, provided that the envelope parameters are scaled as

$$k_{eff}^2 = \frac{\sigma_r}{2\gamma\beta^2} + \left(\frac{qB_z}{\gamma\beta mc} \right)^2 \left. \vphantom{k_{eff}^2} \right\} \Rightarrow \left\{ \begin{array}{l} (\gamma\beta)^{1/2} \sigma_r \\ (\gamma^2 + 2)(\gamma')^2 \\ (\gamma\beta)^{3/2} \epsilon_{eff}^2 \\ (\gamma\beta)^{1/2} \kappa_s \end{array} \right. + \left(\frac{qB_z}{\gamma\beta mc} \right)^2 \quad (12)$$

Emittance Compensation

It has been shown previously [4] that the projected emittance oscillates with the same spatial frequency as the beam envelope. On emission from the photocathode, the beam will contain small fluctuations in equilibrium radius along its length. The different longitudinal beam slices will have different initial phases of the emittance oscillation. For small variations from a nominally matched laminar beam the slices will oscillate together coherently such that the total emittance projected over all the slices has a sinusoidal variation down the beamline [4]

$$\epsilon_{nr} \approx \frac{\gamma\beta}{2\sqrt{2}} k_{eq} \sigma_0 \sigma_{eq} (I_{peak}) \frac{\delta t_{rms}}{I_{peak}} |\sin(k_{eq}z)|. \quad (13)$$

From equation (11), it is seen that the projected emittance minima occurs periodically along the beamline. As the beam accelerates, the emittance value is eventually ‘frozen’ in. Focusing and acceleration profiles for photoinjectors can be determined so that the projected emittance passes through a minima as the beam energy increases to the point that space-charge induced emittance oscillations are negligible.

We study solutions to the envelope equation by parameterizing with respect to the initial angular momentum. The RF gun design may then be considered optimized for a particular value of the initial angular momentum when the effective radial emittance is minimized.

Parameterizing With Cyclotron Phase Advance

We have used HOMDYN [6] to evaluate possible operating points of a flat beam injector. The degree of emittance compensation provided by solenoid focusing can be measured against the cyclotron phase advance, θ_c ,

$$\theta_c(t_{final}) = \int_0^{t_{final}} dt \frac{eB_z}{m\gamma}. \quad (14)$$

This parameter is useful when comparing simulations or experimental data sets when the initial beam spot is held constant. When the spot size varies, the Larmor phase advance,

$$\theta_L(t_{final}) = \int_0^{t_{final}} dt \left(\frac{p_\theta}{m\gamma} \frac{1}{r^2} + \frac{eB_z}{2m\gamma} \right), \quad (15)$$

is the appropriate measure of single particle azimuthal motion. The utility of the cyclotron phase advance is such that it only depends on the solenoid tune and the beam energy. It provides a measure independent of the beam

envelope dynamics, including space charge and emittance effects.

EXPERIMENTAL STUDIES AT FNPL

Experimental studies of flat beam production has been underway at the FNPL (Fermilab-NICADD Photoinjector Laboratory) facility [7]. The layout of the FNPL beamline is shown in Figure 1.

The FNPL photoinjector consists of a 1.6 cell, 1.3 GHz RF gun with a high quantum efficiency Cs₂Te photocathode driven by a frequency-quadrupled Nd:glass laser, followed by a 9-cell superconducting booster cavity resulting in an 14-15 MeV electron beam. A dipole chicane is present to provide magnetic bunch compression. As shown in Figure 1, three of the normal quadrupoles have been rotated about their axis to become skew quadrupoles. During flat beam production, these skew quadrupoles are energized.

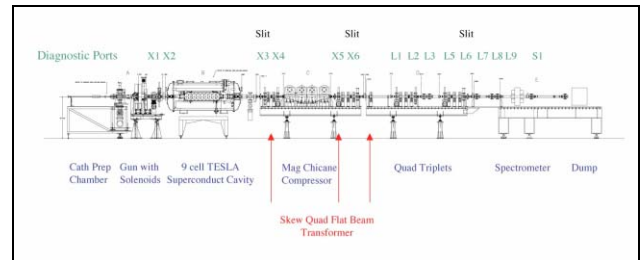


Figure 1: FNPL beamline.

Emittance Optimization Studies

Parametric studies were performed to examine the effect of solenoid focusing on flat beam final emittance and emittance ratio. The main solenoid provides the field on the cathode and defines the initial canonical angular momentum on the beam. The secondary solenoid controls the matching into the booster accelerator and tunes for emittance compensation.

The cyclotron phase advance at the entrance to the booster module has been calculated using HOMDYN. Figure 2 shows the cyclotron phase advance (in units of π) as the secondary solenoid current is varied over its full range, for different values of the main solenoid current. By varying the current in both the main and secondary solenoids a usable range of cyclotron phase advance from $\sim 0.8\pi$ to $\sim 1.5\pi$ radians can be explored.

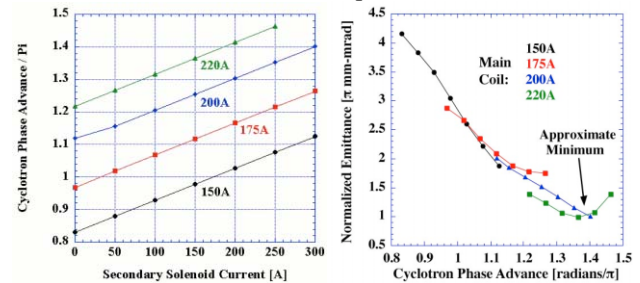


Figure 2: HOMDYN simulations: (left) Cyclotron phase advance (in units of π) vs. secondary solenoid current, (right) Normalized emittances at the booster exit.

Beam envelopes and radial emittances from HOMDYN simulations for four distinct cyclotron phase advances (0.88π , 1.1π , 1.35π , 1.46π) are shown in Figure 3.

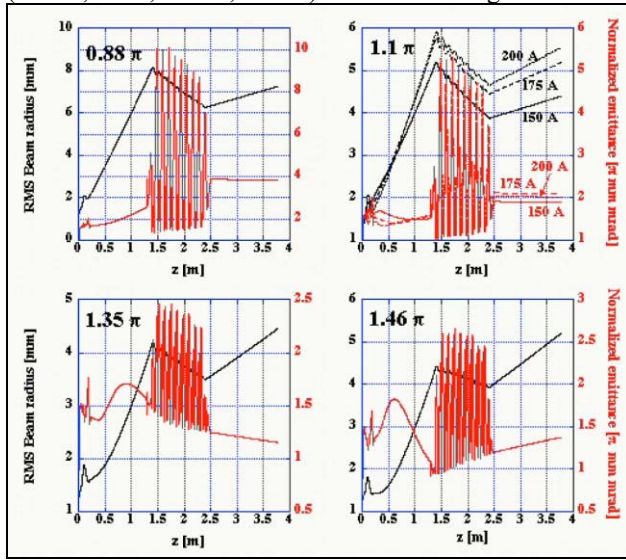


Figure 3: Beam envelope (black) and radial emittance (red) for cyclotron phase advances of 0.88π , 1.1π , 1.35π , and 1.46π (HOMDYN).

In the first two regions (cyclotron phase advance of 0.88π and 1.1π) the beam is under-compensated, the emittance increases through the booster. In the second region (1.1π), the emittance at the exit of the booster is reduced by a factor ~ 2 compared to the previous case.

We see here the utility of cyclotron phase as a measure of emittance compensation. The results of three separate simulations, with different values of angular momenta, but with equal cyclotron phase advance (1.1π) are overlaid. The beam envelopes show some difference, but the emittance evolution is identical for the three cases.

The third (1.35π) case shows the emittance compensated case, while the fourth (1.46π) cases shows the over-compensated case in which the emittance oscillation has already passed through a minimum before exiting the booster.

Experimental Vertical Emittance Measurement

The vertical emittance at the entrance to the skew quad channel has been measured using the horizontal slit analyzer at the booster cavity module exit and the imaging the beamlets on downstream OTR foils. The measured values are shown in Figure 4. Over the range of parameters scanned, and by comparison with Figure 2 above, we see that the individual emittance minima occur for nearly equal values of the cyclotron phase advance as calculated by HOMDYN.

The absolute values of the emittance are properly to be recognized as upper bounds, as they reflect the projected emittance averaged over approximately 20 bunches with varying bunch charge (~ 0.5 - 1.2 nC per bunch), and hence varying compensated emittance values. These studies will continue with more stringent control over the bunch train charge profile.

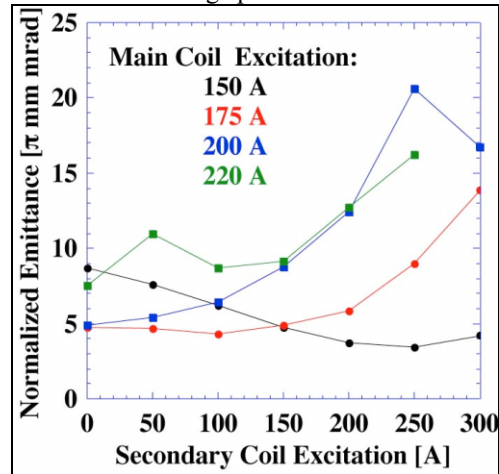


Figure 4: Measured vertical emittances of angular momentum-dominated beam at FNPL.

ACKNOWLEDGMENTS

The author would like to acknowledge the assistance of Kai Desler, James Santucci, and Yin-e Sun during the measurements, and to Helen Edwards for support for these studies.

REFERENCES

- [1] J. Corlett, et.al., "A Recirculating Linac-Based Facility for Ultrafast X-ray Science", *Proceedings of the 2003 Particle Accelerator Conference*, Portland, 2003.
- [2] R. Brinkmann, et. al., 'A Flat Beam Electron Source for Linear Colliders', TESLA 99-09, DESY-Hamburg, 1999.
- [3] B.E. Carlsten, Nucl. Instrum. Methods Phys. Res. A **285**, 313 (1989).
- [4] L. Serafini and J.B. Rosenzweig, Phys. Rev. E, **55**, 7565 (1997).
- [5] Martin Reiser, Theory and Design of Charged Particle Beams, Wiley, New York, 1994.
- [6] M. Ferrario, et. al., Part. Accel., **52**, 1 (1996).
- [7] J.P. Carneiro, et. al., 'Beam transport, acceleration and compression studies in the Fermilab high-brightness photoinjector', *Proceedings of the XIX International Linac Conference*, Chicago, 1998.